



Wei-Ya Su* and Pei-Ying Patty Lin
蘇微雅、林佩瑩

*✉ su0988846561@gmail.com Department of Earth Sciences, National Taiwan Normal University



NOR1-0040 Cruise Experience

1 SALUTE project

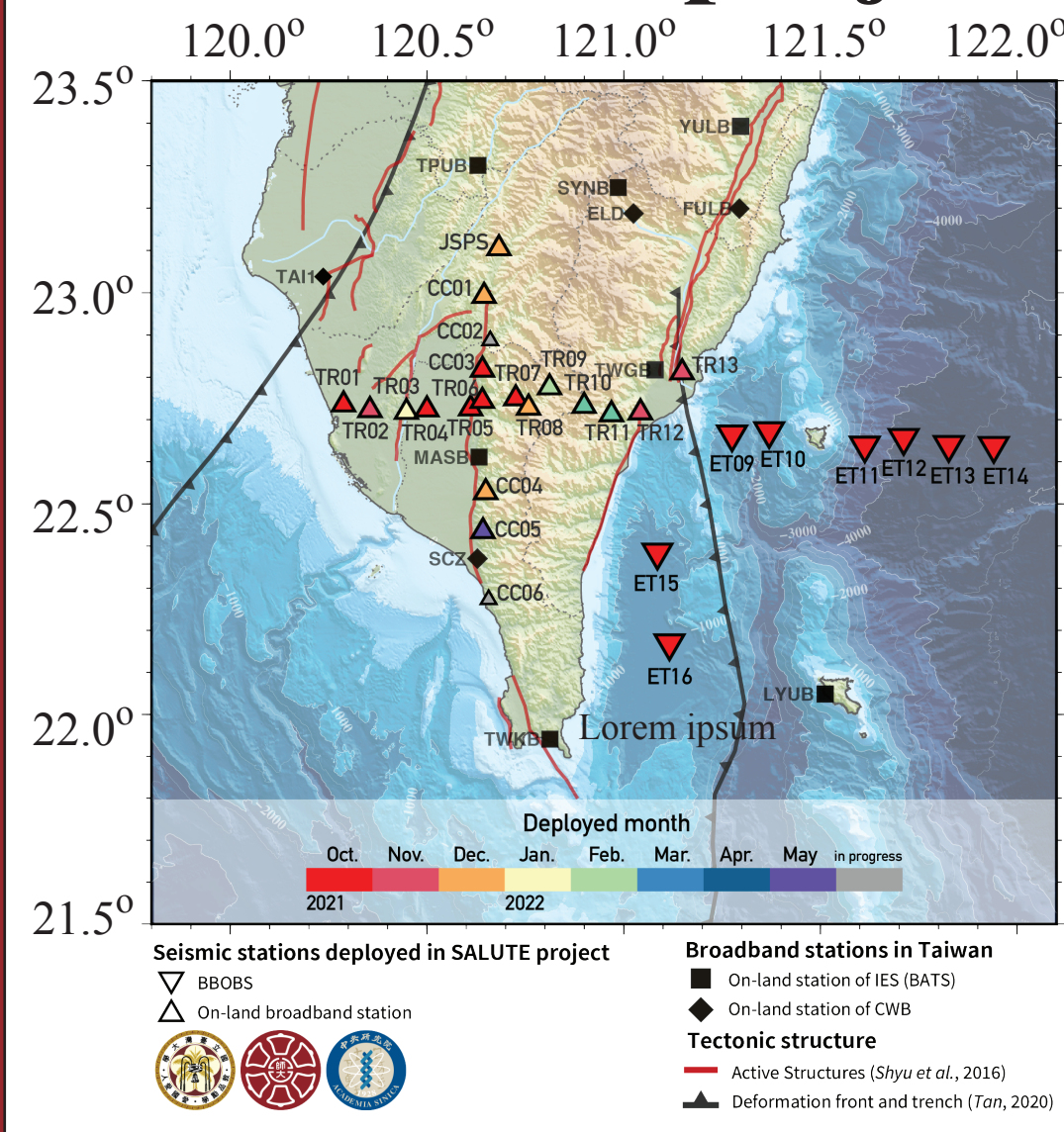


Fig. 1. Distribution map of the in-land stations and the OBSs of SALUTE project.

The Southern Array for the Lithosphere and Uplift of Taiwan Experiment (SALUTE) consists of a totally of 19 in-land broadband seismic temporary stations and 8 broadband ocean bottom seismographs (OBS) formed two-cross-shaped passive seismic array.

2 A cruise with multi-projects

We spent 10 days from 8/18- 8/27 offshore eastern Taiwan. Several tasks were completed including

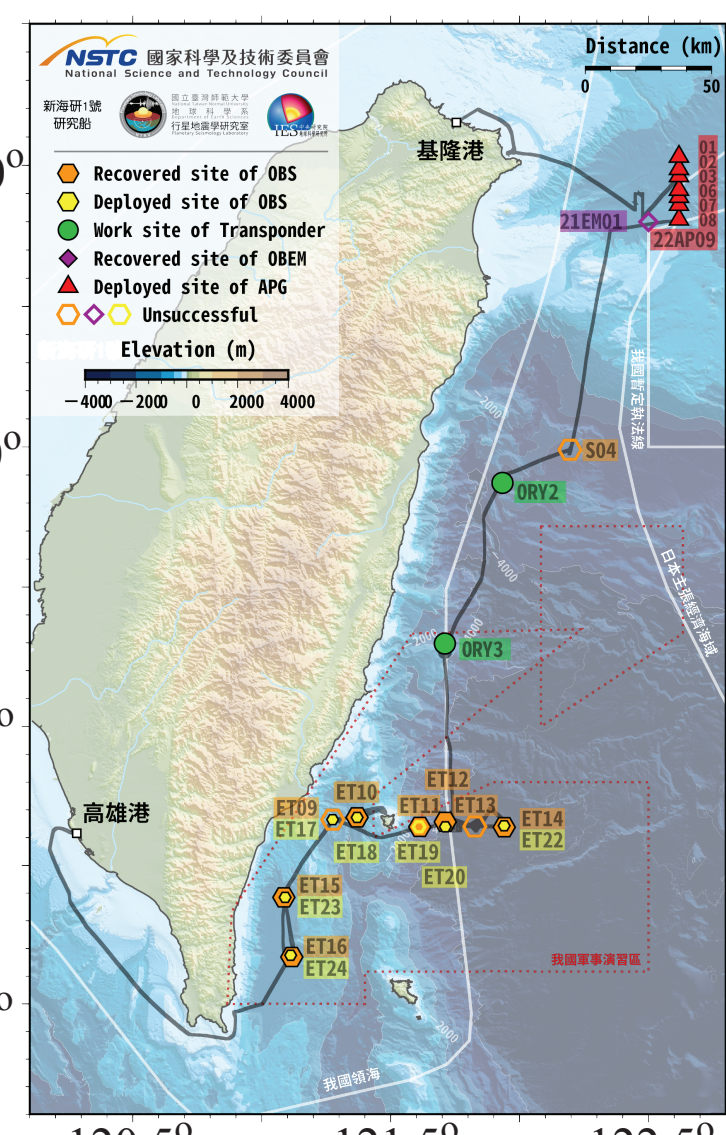


Fig. 2. The cruise track map for the R/V NORI-0040.

- ▶ 7 absolute pressure gauge deployed,
- ▶ geodetic survey for 2 sites,
- ▶ 6 out of 8 BBOBSs recovered, &
- ▶ 6 BBOBSs successfully deployed.

3 OBS- Ocean Bottom Seismograph

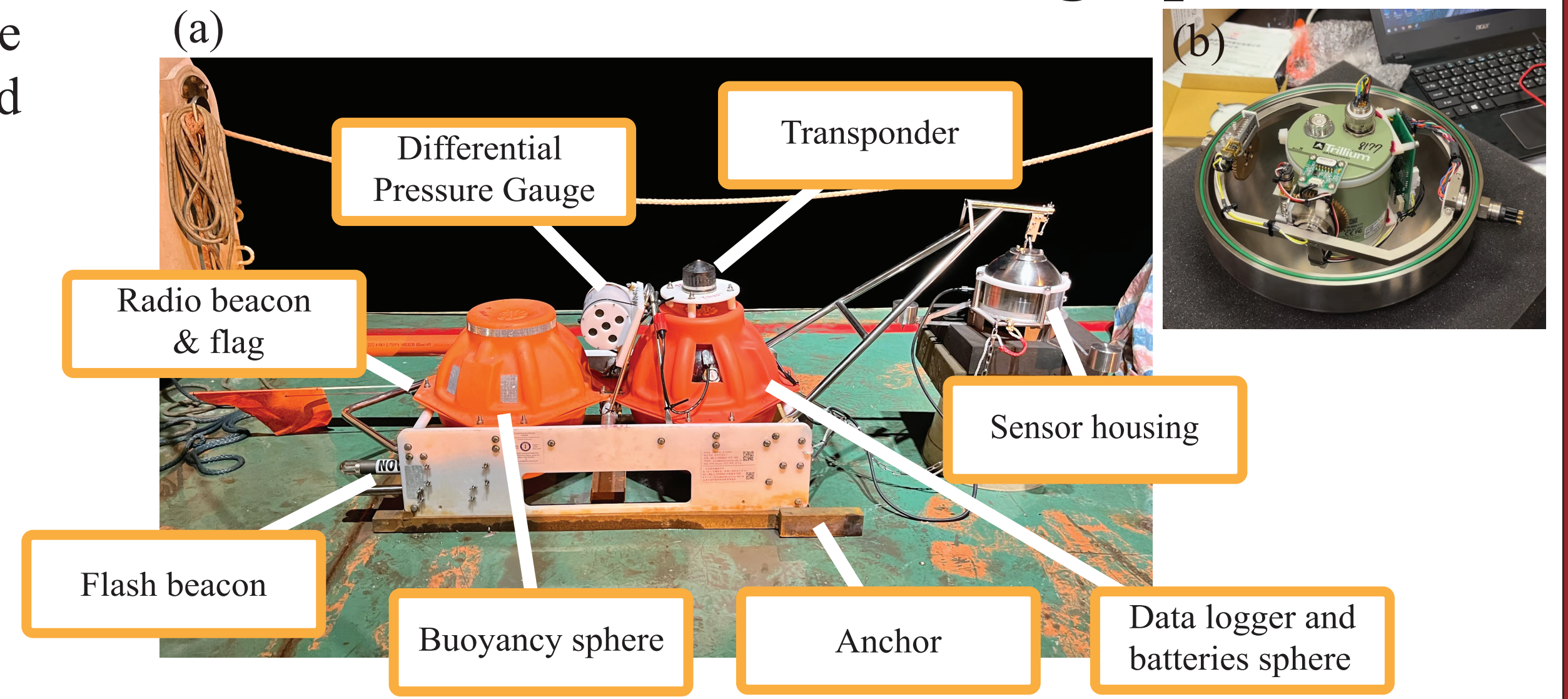


Fig. 3. (a) OBS deployed in SALUTE experiment with main instrument components indicated. (b) The inside of sensor housing. The sensor is trillium compact 120s which measures the ground motion and transmits signals to the data logger.

North Okinawa Trough (NOT) OBS dataset

The NOT experiment was conducted in order to understand the dynamics of the Ryukyu subduction system as a collaboration between Taiwan and Japan. The data of 30 BBOBSs and 8 in-land stations are used in this study.

Free-drop deployed OBS data often recorded 2 significant noises (Fig. 5) which will contaminated with true seafloor motions (Fig. 6). Tilt noise mainly is due to the coupling problems and the ocean bottom current. The compliance noise which mainly due to long-period (> 30 s) ocean waves. After correcting, the clear P, S, and Rayleigh waves can be observed.

5.2 Main noises recorded in OBS

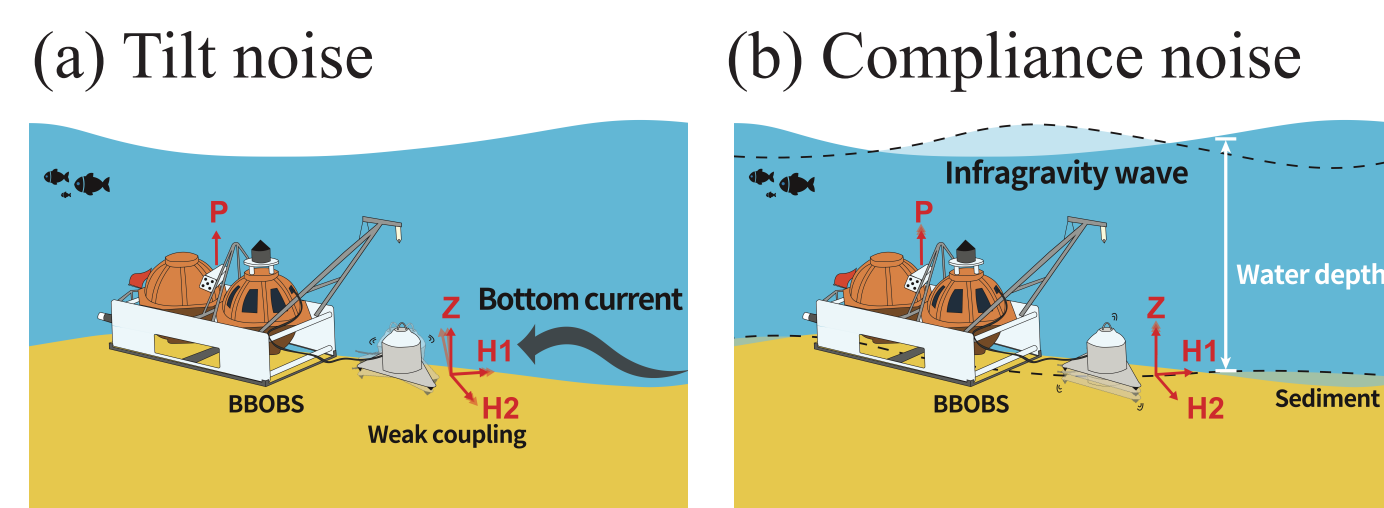


Fig. 5. The cartons for (a) tilt and (b) compliance noises, respectively (modified from Lin et al., 2022).

6 Noise corrections for Z component waveforms

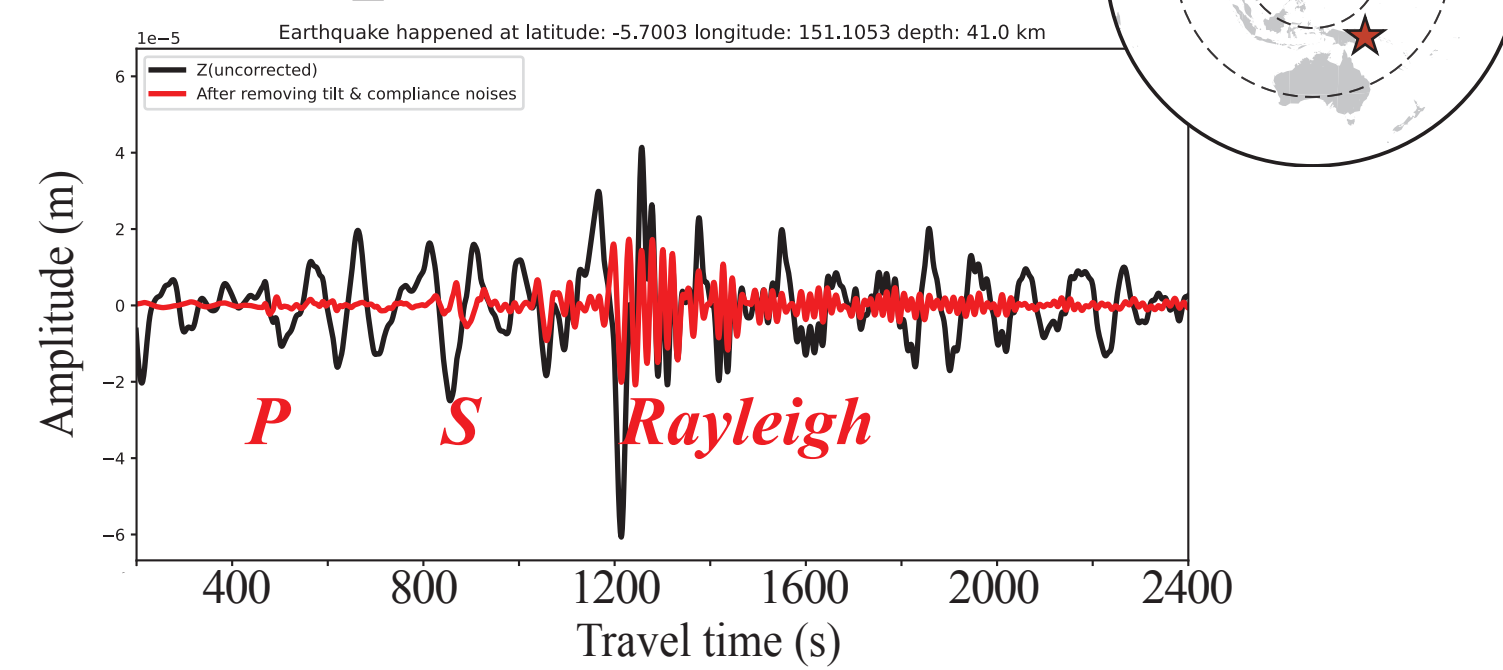


Fig. 6. The vertical (Z) waveforms of the earthquake occurred on 2019/03/30 and filtered at 15-100 s. The black line is uncorrected waveform. The red line is after removing tilt and compliance noises.

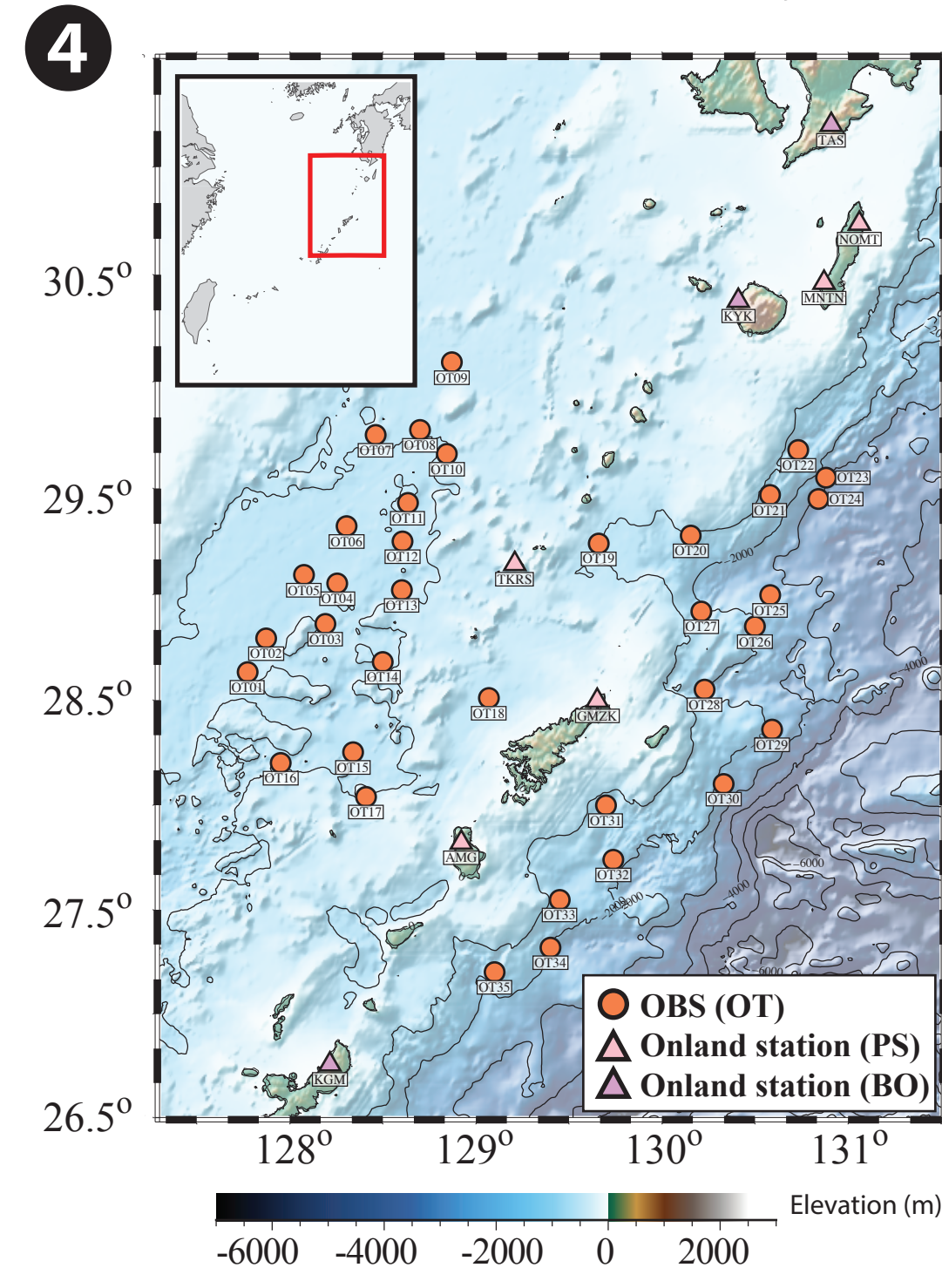


Fig. 4. Distribution map of the OBS (circles) and on-land station (triangles) used in this study. The operation is during 2018/09/05- 2019/06/25. The array aperture spans ~ 600 km x 400 km.

Results

We measured the frequency-dependent phase delays between all possible nearby station pair (Fig. 11a) via cross-correlation. The Rayleigh-wave dispersion characteristics are clearly observed (Fig. 11b).

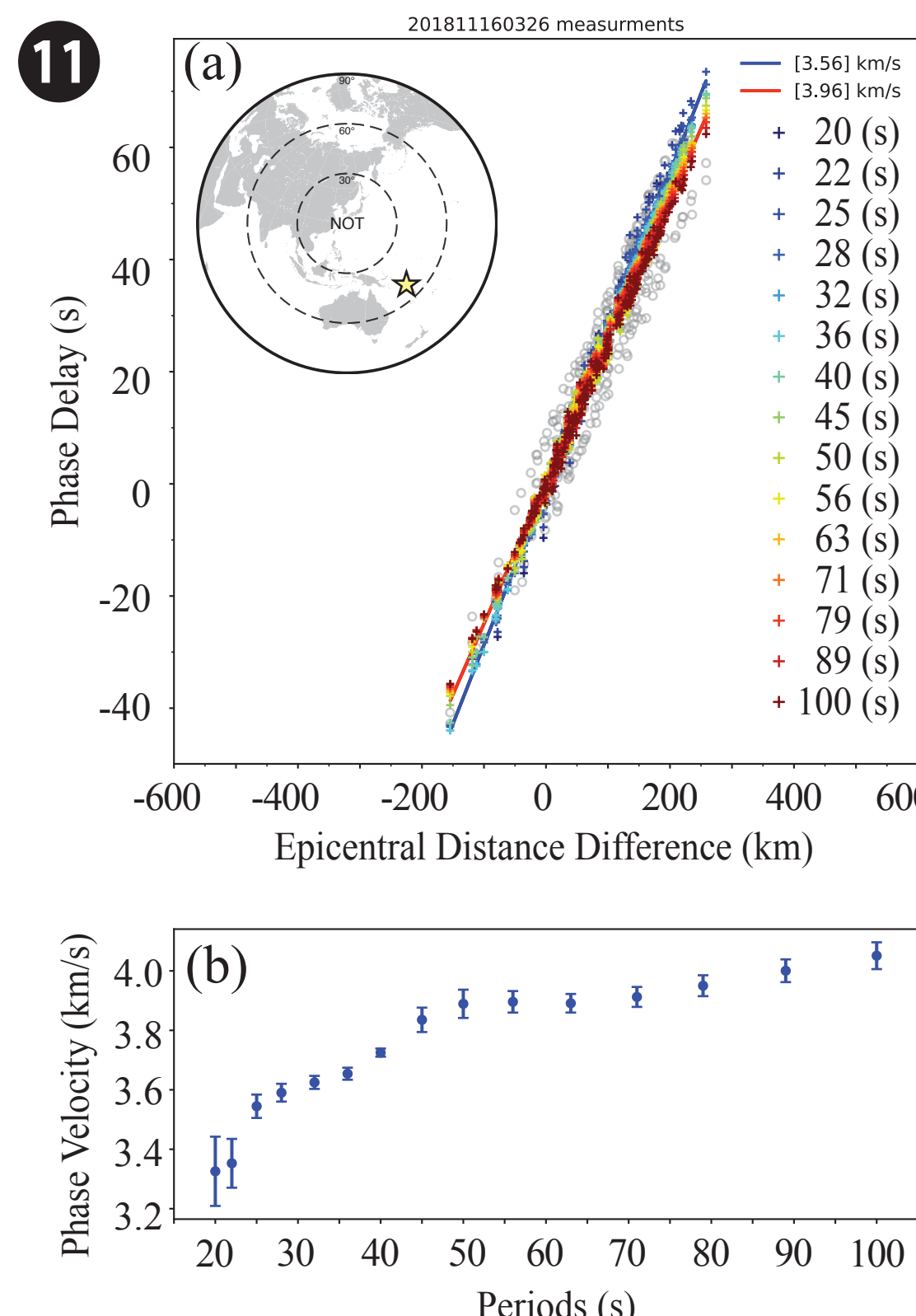


Fig. 11. (a) Relative phase delays versus epicentral distance difference for all the station pairs for the 2009 January 18, earthquake. Crosses with different color represent the measurements at different periods. Gray circles are discarded measurements. (b) The dispersion curve estimated by the slope of each line in (a) for different periods.

12 Phase velocity structure

The preliminary results of stacked apparent phase velocity maps at different periods (T) are obtained by stacking the apparent phase-velocity maps from 27 earthquakes. The stacked phase-velocity maps show the lateral variations at different periods. Higher frequency Rayleigh waves sample shallower structures, with the depth of maximum sensitivity being roughly one-third of the wavelength.

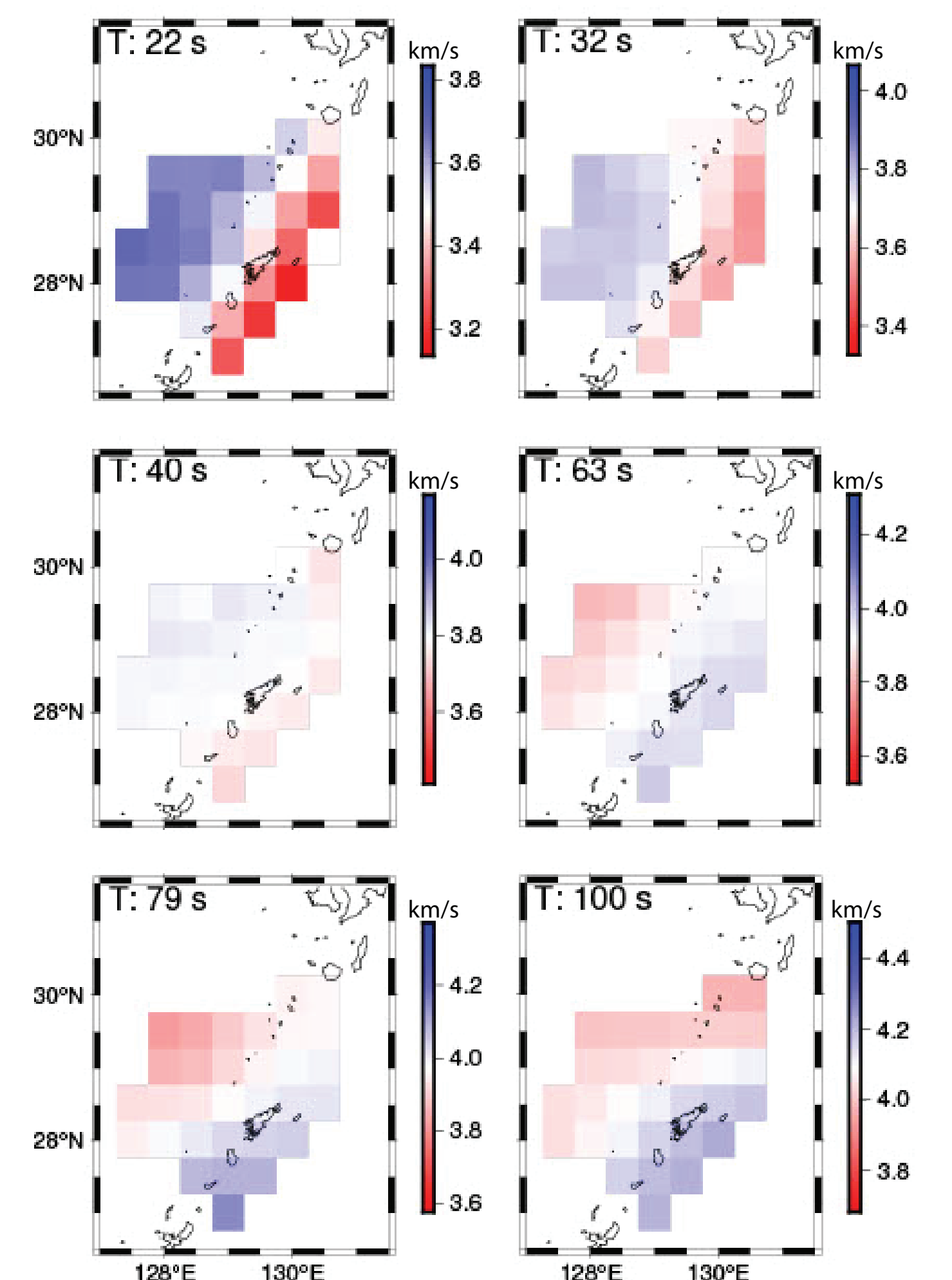


Fig. 12. Rayleigh-wave phase-velocity maps at different periods, with 27 events stacked.

Measuring the Phase Velocity of Surface Waves

Surface-wave dispersions

Surface waves dispersed because different periods waves travel in different speed (Fig. 7). Different periods provides sensitivity to different depths. Phase velocity can be estimated the slope of the individual peaks of the Rayleigh waves (Fig. 8).

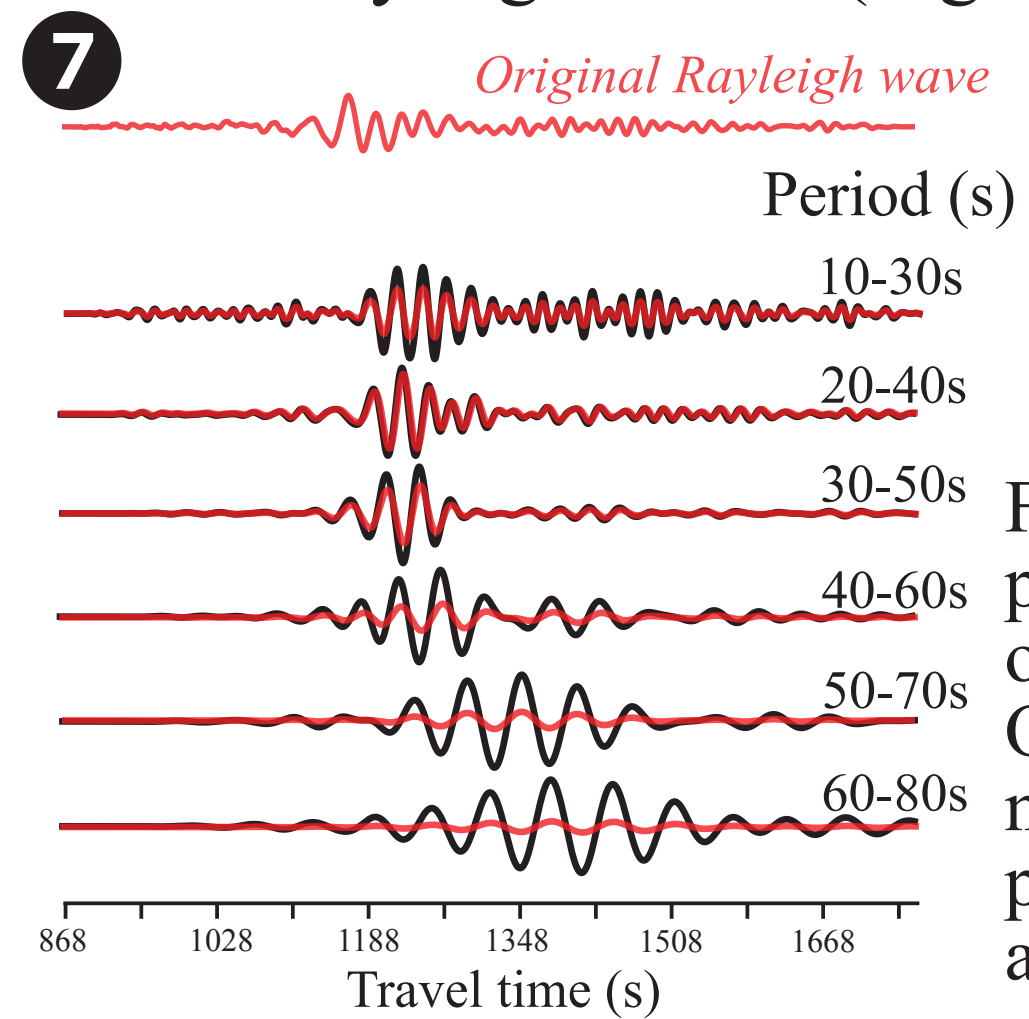


Fig. 7. Example for dispersion characteristics of surface waves in Z of OBS OT02. The original and normalized amplitude are plotted in red and black respectively.

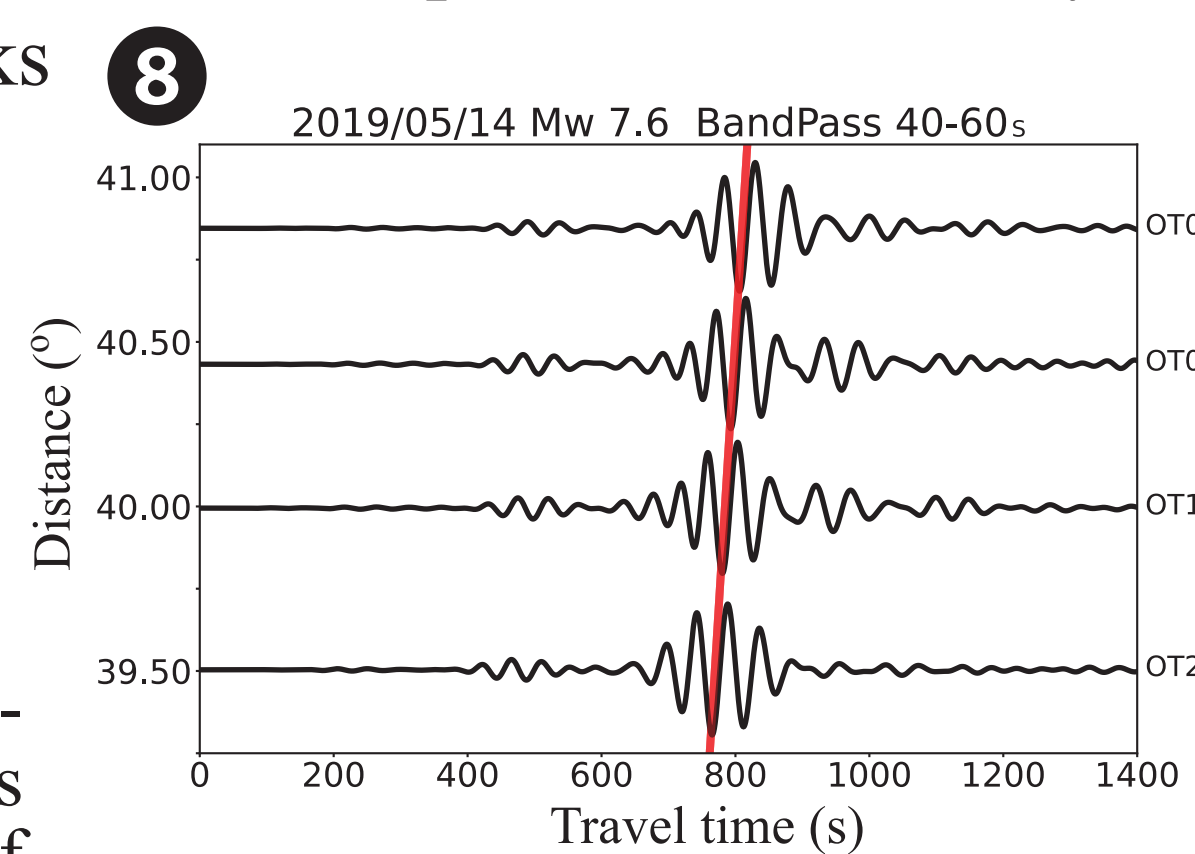


Fig. 8. The Z waveforms filtered at 40-60s for the Rayleigh waves recorded in OBSs OT07, OT02, OT14 and OT21. The phase velocity can be estimated the slope of the individual peaks as shown in the red line.

Intra-array cross-correlation

The coherence in waveforms between adjacent stations results in highly precise delayed time (Fig. 9). We applied cross-correlation to get the lag time (s) through the lag of maximising the coherence. The phase-delay time between any two stations shows the slowness vector propagated between the stations (Fig. 10).

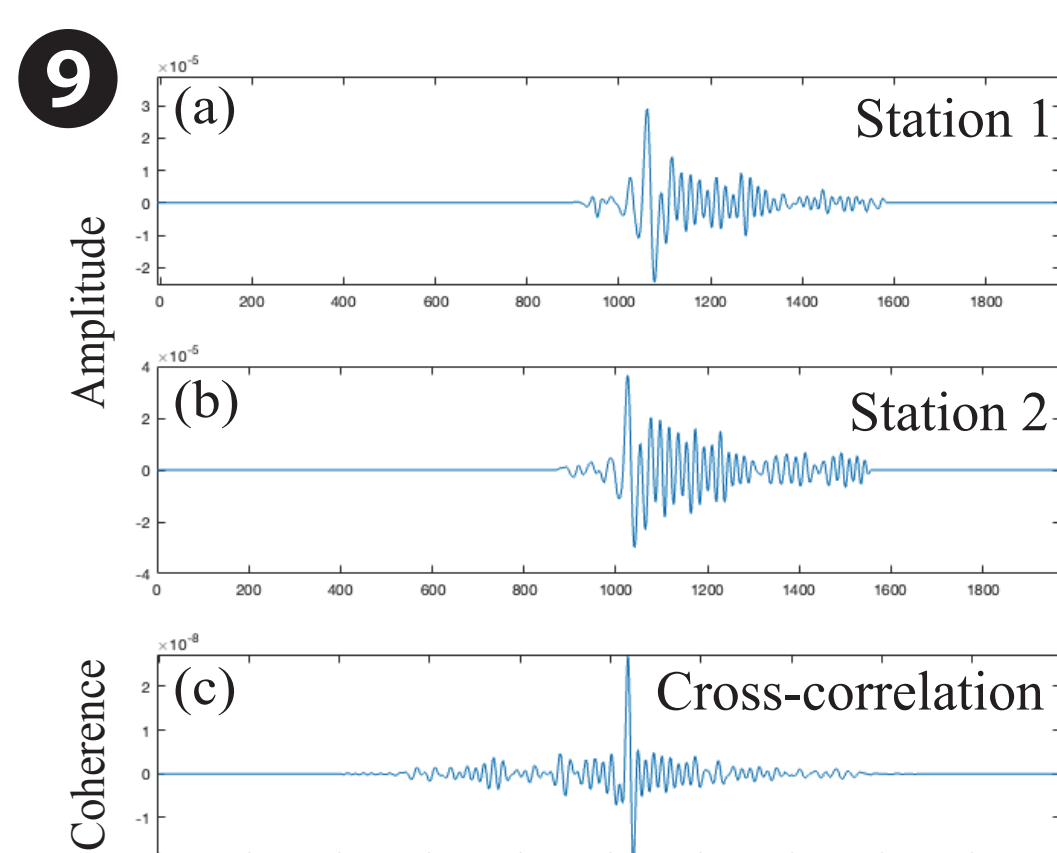


Fig. 9. (a) and (b) are the sample waveforms from a nearby station pair. (c) Cross-correlation processing of Rayleigh waves.

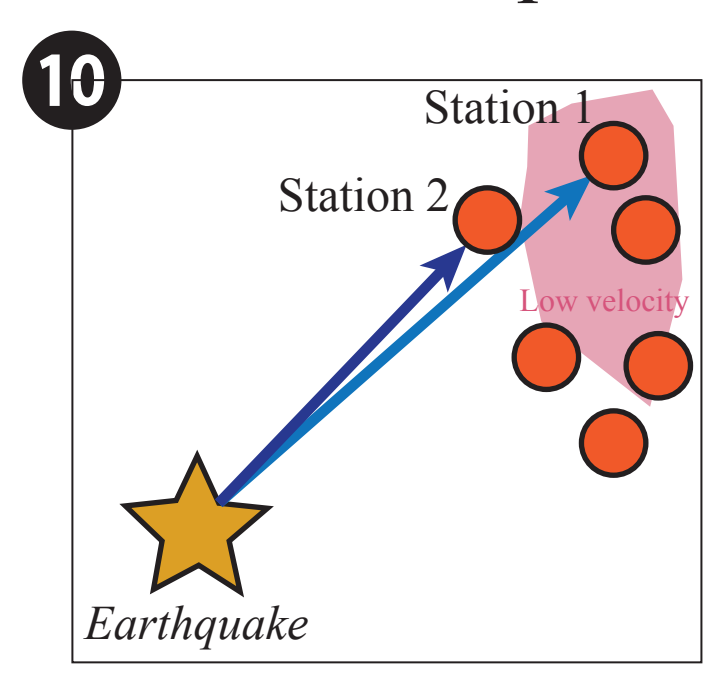


Fig. 10. The cartoon concepts of intra-array methodology.

Key Points & Future Perspectives

- From my experiences of preparing and joining the research cruise, I deeply realized that the data collected in the inner space are treasure.
- Although the noise level is higher in OBS data than onland stations, the signals measured on the seafloor can be enhanced after the reduction of tilt and compliance noises.
- We utilize an intra-array cross-correlation analysis to estimate the average Rayleigh waves dispersion in this region. The phase velocities are ~ 3.4 m/s in shorter period and are higher, ~ 4.1 m/s, in longer period.
- The Rayleigh-wave phase velocity maps show the lateral variations for different periods. For shorter periods, the fast lithospheric lid appeared in the Okinawa Trough. For longer periods, the fast anomalies showed which might be associated with the subducted Ryukyu slab.
- The result of Rayleigh-wave phase velocity structure will be used to invert the shear velocity structure in order to understand the dynamics of the Ryukyu subduction system.

References

Jin, G. and Gaherty, J. B. (2015). *Geophysical Journal International*, 201(3), 1383-1398.
Lin, C.-M., Lin, P.-Y. P., Yeh, H.-C., and Kuo, B.-Y. (2022). *Taiwan Geosciences Assembly (TGA)*, Taiwan, GS19-014. (Oral).

Acknowledgements

